DOI: 10.1002/chem.200801802

Peripheral Hexabromination, Hexaphenylation, and Hexaethynylation of *meso*-Aryl-Substituted Subporphyrins

Eiji Tsurumaki,[a] Yasuhide Inokuma,[a] Shanmugam Easwaramoorthi,[b] Jong Min Lim,[b] Dongho Kim,*[b] and Atsuhiro Osuka*[a]

Abstract: Effective peripheral fabrication methods of *meso*-aryl-substituted subporphyrins were explored for the first time. Hexabrominated subporphyrins **2** were prepared quantitatively from the bromination of subporphyrins **1** with bromine. Hexaphenylated subporphyrins **3** and hexaethynylated subporphyrins **4** and **5** were synthesized by Suzuki–Miyaura coupling and Stille coupling, respectively, in good yields. X-ray crystal structures of **2b**, **3b**, **4b**, and **5a** revealed preservation of the bowl-shaped bent structures with bowl depths similar to that of **1**. Hexaethynylated subporphyrins exhibit large two-photon-absorption cross-sections due to effective delocalization of the conjugated network to the ethynyl substituents.

Keywords: bromination · cross-coupling · porphyrinoids · structure elucidation · subporphyrins

Introduction

Subporphyrin is a genuine ring-contracted porphyrin that has C_{3v} molecular symmetry and a 14π-electronic-conjugated network.[1] This macrocycle has been long elusive despite its key position in porphyrin chemistry, however, since our first synthesis in 2006[2] it has emerged as a promising functional pigment owing to its intense Soret-like absorption band, bright-green fluorescence, and aromaticity along the unique bent-bowl-shaped structure. The chemistry of subporphyrins contrasts sharply with that of subphthalocyanines, which has been continuously and extensively studied since their serendipitous synthesis by Meller and Ossko in 1972.[3,4]

Although the attractive features of subporphyrins suggests they have promising potential,[5–7] the chemistry of subporphyrin still remains largely unexplored, due mainly to poorly developed synthetic methodology able to produce subporphyrins or to fabricate their peripheries. Herein we report the effective perbromination and subsequent coupling reactions of subporphyrins as the first peripheral fabrications of subporphyrins. Similar synthetic protocols have been extensively explored for porphyrins.[8–11]

In the chemistry of subphthalocyanine and subporphyrazine, peripheral fabrications have been widely used for chromophore tuning or attachment of synthetic handles. Taking advantage of versatile phthalonitrile precursors, peripherally halogenated,[12a,b] arylated, thioalkylated,[12c,13] nitrated,[12d] and ethynylated[14] subphthalocyanines with diverse electronic properties have been synthesized. In contrast, such synthetic procedures are unknown for subporphyrins, and hence the peripheral fabrication reactions reported here are significant and should provide a useful synthetic platform for further functionalizations of subporphyrins.

Results and Discussion

Synthesis: *meso*-Triaryl-substituted subporphyrins **1a** and **1b** were prepared by our synthetic protocol,[6a] which was based on the condensation of pyridine-tri-*N*-tripyrrolylborane (PPB)[15] and aromatic aldehyde. In the initial paper,[15a] PPB was synthesized from tri-*N*-pyrrolylborane (PB). Although the yield was acceptable, it was quite troublesome to scale-up the synthesis, due mainly to the instability of PB, especially towards moisture. Therefore, tedious sublimation was required for purification of PB, which had to be per-

[a] E. Tsurumaki, Y. Inokuma, Prof. Dr. A. Osuka
Department of Chemistry, Graduate School of Science
Kyoto University, Sakyo-ku, Kyoto 606-8502 (Japan)
Fax: (+81) 75-753-3970
E-mail: osuka@kuchem.kyoto-u.ac.jp

[b] Dr. S. Easwaramoorthi, J. M. Lim, Prof. Dr. D. Kim
Center for Ultrafast Optical Characteristics Control and
Department of Chemistry, Yonsei University, Seoul 120-749 (Korea)
Fax: (+82) 2-2123-2434
E-mail: dongho@yonsei.ac.kr

Supporting information for this article is available on the WWW under http://dx.doi.org/10.1002/chem.200801802.

formed in a glove-box. We found that the reaction of pyrrole and borane-triethylamine according to the procedure reported by Köster et al.[15b] afforded almost pure PB that can be used for the preparation of PPB without further purification. Namely, a mixture of borane-triethylamine and 3 equiv of freshly distilled pyrrole was heated to 100 °C under N_2 atmosphere for 2.5 h; subsequent removal of triethylamine by heating at 160 °C left crude PB as a pale-yellow cake. This crude product was dissolved in pyridine at 100 °C and then cooled to room temperature to provide pure PPB as a colorless crystalline solid in 64 % yield. This improved procedure allowed us to prepare PPB on a 50–60-g scale from commercially available borane-triethylamine complex. Regarding the characterization of PPB, only the elemental analysis was reported in the literature,[15a] so we have completed characterization by ^{1}H, ^{11}B, and ^{13}C NMR spectroscopy and X-ray crystallographic analysis. This improved synthesis of PPB is useful as it helps provide a substantial amount of subporphyrins (1–2-g scale) in a few steps from the commercially available compounds.

In the solid state, PPB exhibits B–N(pyrrole) distances in the range of 1.52–1.53 Å, and a B–N(pyridine) distance of 1.63 Å, suggesting covalent- and coordination-bond characters, respectively (Figure 1). PPB is a robust molecule under

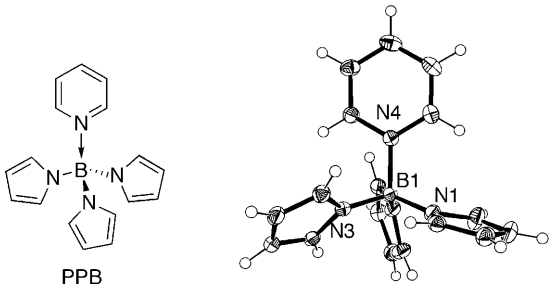

Figure 1. X-ray crystal structure of pyridine-tri-*N*-pyrrolylborane (PPB).

aerobic and wet conditions, much superior to PB. Usually, PPB can be handled easily, although being exposed to air over a week caused dark brown coloration. Subporphyrins **1a** and **1b** were prepared from PPB by our modified Adler protocol involving an additional oxidation step with activated MnO_2.[6c] As an initial attempt, bromination of **1a** with *N*-bromosuccinimide (NBS) was examined under various conditions. A solution of **1a** in bromobenzene was refluxed in the presence of 60 equiv NBS and the progress of reaction was monitored by MALDI-TOF mass spectroscopy. Mono-, di-, and tribrominated products formed quickly, but further brominations were found to be rather sluggish. After refluxing for five days, the bromination was almost completed, giving hexabrominated subporphyrin **2a** in more than 90 % yield. Although the ^{1}H NMR spectrum of the reaction mixture was almost pure, showing disappearance of β-proton signals around $\delta = 8.1$ ppm, the high-resolution electrospray-ionization time-of-flight (HR ESI-TOF) mass spectrometry revealed the contamination of incomplete bromination products that turned out to be very difficult to separate. As a more reliable and effective method, we found that bromination of **1a** with bromine at room temperature for 2 h afforded **2a** quantitatively after usual work-up without tedious separation (Scheme 1). HR ESI-TOF mass spectrometry revealed a parent molecular-ion peak of **2a** at *m*/*z* 943.6395 (calcd for $C_{33}H_{15}N_3Br_6B_1 = 943.6402$, $[M-OMe]^+$). In the ^{1}H NMR spectrum of **2a**, the β-proton signal completely disappeared and only a single signal set of *meso*-aryl groups was observed in the aromatic region. This indicates that bromination occurred selectively at the periphery preserving C_3 molecular symmetry. The ^{1}H NMR spectrum of **2a** also shows restricted rotation of the *meso*-phenyl substituents by exhibiting broad but clearly split signals due to the *ortho* protons at $\delta = 8.03$ and 7.34 ppm and the *meta* pro-

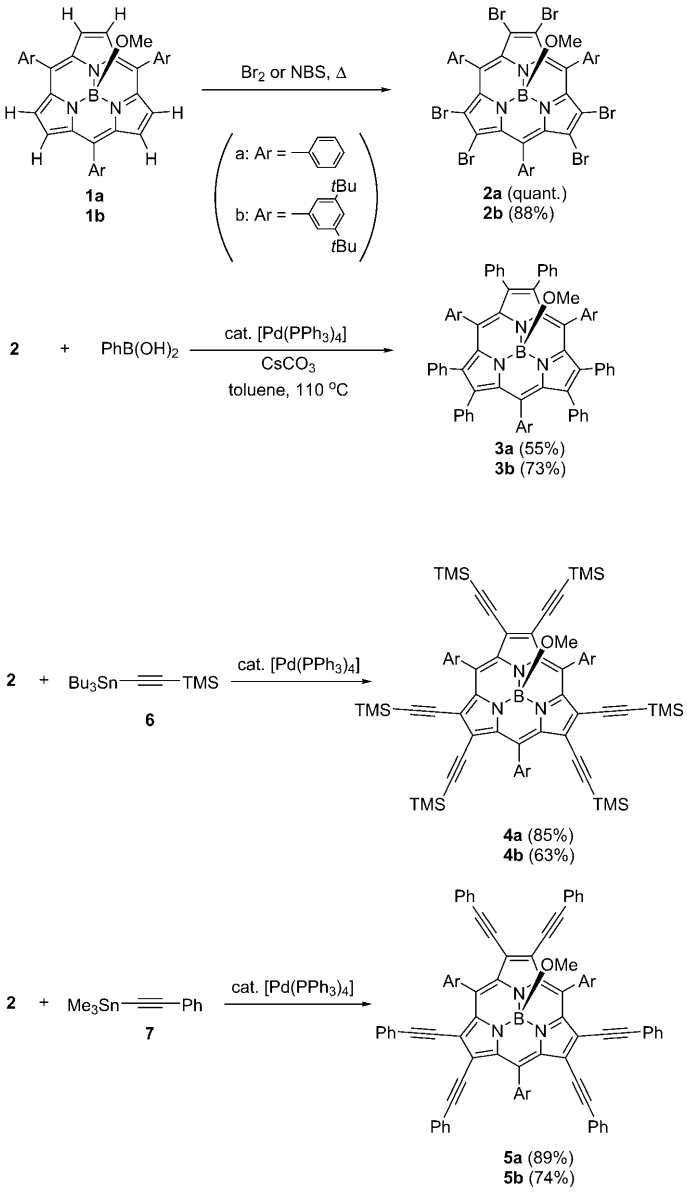

Scheme 1. Synthesis of peripherally subsitituted subporphyrins **2**–**5**.

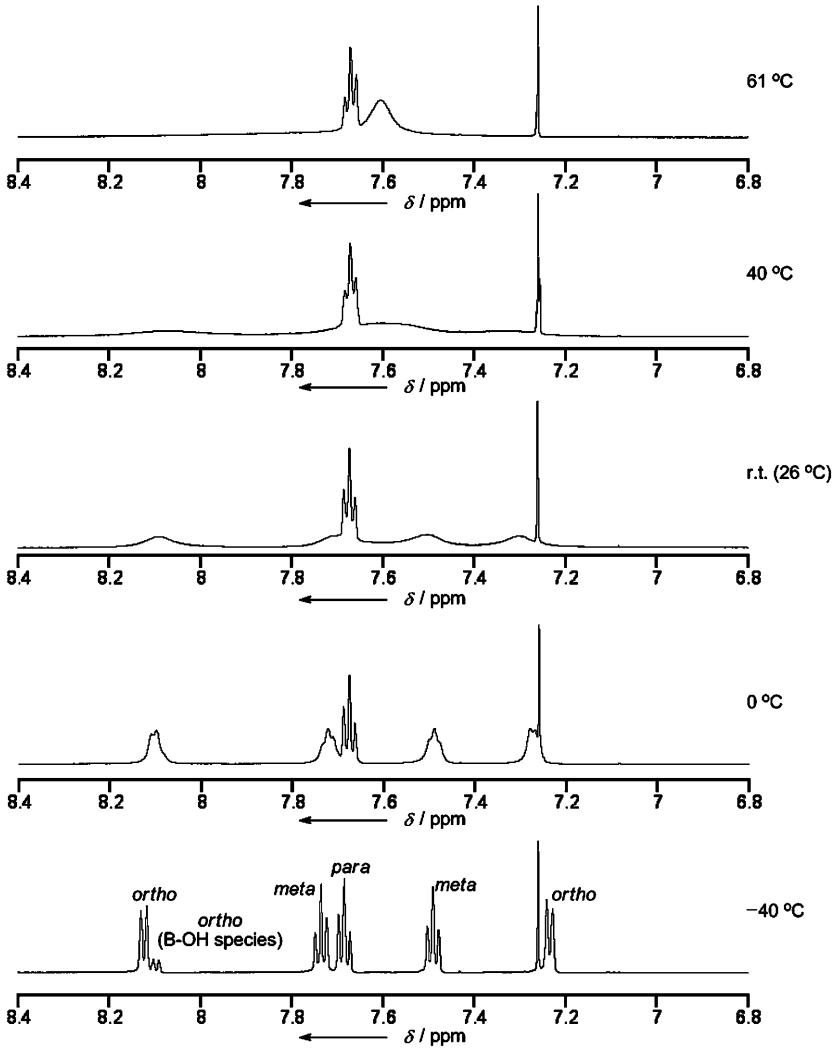

Figure 2. Temperature-variable 600 ^{1}H NMR spectra of **2a** in $CDCl_3$.

tons at $\delta = 7.70$ and 7.50 ppm at room temperature (Figure 2). Similarly, perbrominated subporphyrin **2b** was prepared in 88% from the reaction of **1b** with bromine (Scheme 1).

In next step, we examined the coupling reactions of **2a** and **2b** at the periphery. Suzuki–Miyaura coupling reaction of **2a** with phenyl boronic acid under the standard conditions ($[Pd(PPh_3)_4]$, K_2CO_3 (60 equiv), toluene, 110 °C, 5 days) provided hexaphenylated product **3a**. ^{1}H NMR analysis of the reaction mixture indicated the formation of a hexaphenylated product as a major product, however, the presence of a small amount of a pentaphenylated product hampered the isolation of pure **3a** due to separation difficulty. Actually, the isolation yield of pure **3a** in this run was low (ca. 17%) after repeated silica-gel column chromatography. To complete the phenyl coupling, the above reaction mixture was once again subjected to the same bromination and Suzuki–Miyaura coupling reaction under similar conditions. After this treatment, **3a** was isolated in 55% yield after usual work-up (Scheme 1). Following the same procedure, hexaphenylated subporphyrin **3b** was obtained in 73% yield. Although **3a** exhibits poor solubility in common organic solvents such as CH_2Cl_2, $CHCl_3$, and THF, **3b** displays much better solubility. In the HR ESI-TOF mass spectra, the parent-ion peaks of **3a** and **3b** were observed at *m*/*z* 926.3710 and 1262.7470, which matched the expected values, 926.3712 for $C_{69}H_{45}N_3B_1$ $[M-OMe]^+$, and 1262.7471 for $C_{93}H_{93}N_3B_1$ $[M-OMe]^+$. As seen for **2**, **3a**, and **3b** exhibit a single signal set of *meso*- and β-aryl groups in their ^{1}H NMR spectra, thus suggesting the preservation of C_{3v} molecular symmetry.

Next, Stille coupling reactions of **2a** and **2b** were examined using ethynes **6** and **7**. Under typical reaction conditions ($[Pd(PPh_3)_4]$ (0.6 equiv), THF), Stille reactions of **2a** with both **6** and **7** proceeded smoothly at 70 °C, yielding **4a** and **5a** in 89 and 85% yields, respectively (Scheme 1). On the other hand, the Stille reactions of **2b** with **6** and **7** proceeded only at higher temperature, 110 °C, to provide subporphyrins **4b** and **5b** in 63 and 74% yields, respectively (Scheme 1). Note that Sonogashira coupling reaction of **2a** with trimethylsilylacetylene afforded an intractable mixture containing nona-, deca-, undeca-, and dodeca-substituted products,[16] as revealed by MALDI-TOF analysis. The borenium cation peaks were detected by HR ESI-TOF mass spectrometry at 1046.4206 for **4a** (calcd for $C_{63}H_{69}N_3B_1Si_6$ = 1046.4206 $[M-OMe]^+$), 1389.7987 for **4b** (calcd for $C_{97}H_{117}N_3B_1Si_6$ = 1383.7982 $[M-OMe]^+$), 1070.3705 for **5a** (calcd for $C_{81}H_{45}N_3B_1$ = 1070.3714 $[M-OMe]^+$), and 1407.7499 for **5b** (calcd for $C_{105}H_{93}N_3B_1$ = 1407.7499 $[M-OMe]^+$).

X-ray diffraction analysis: The solid-state structure of **2b** was revealed by single-crystal X-ray diffraction analysis to be bowl-shaped (Figure 3 and Table 1). The structural data of **1b** is also listed for comparison. Bowl depth, defined as the distance between the boron atom to the mean plane of the six β carbons, is 1.24 Å for **2b**, which is slightly shorter than that of **1b** (1.29 Å). Bond lengths of B–N and B–O in **2b** are 1.491(6), 1.507(7), 1.489(6), and 1.452(6) Å, which

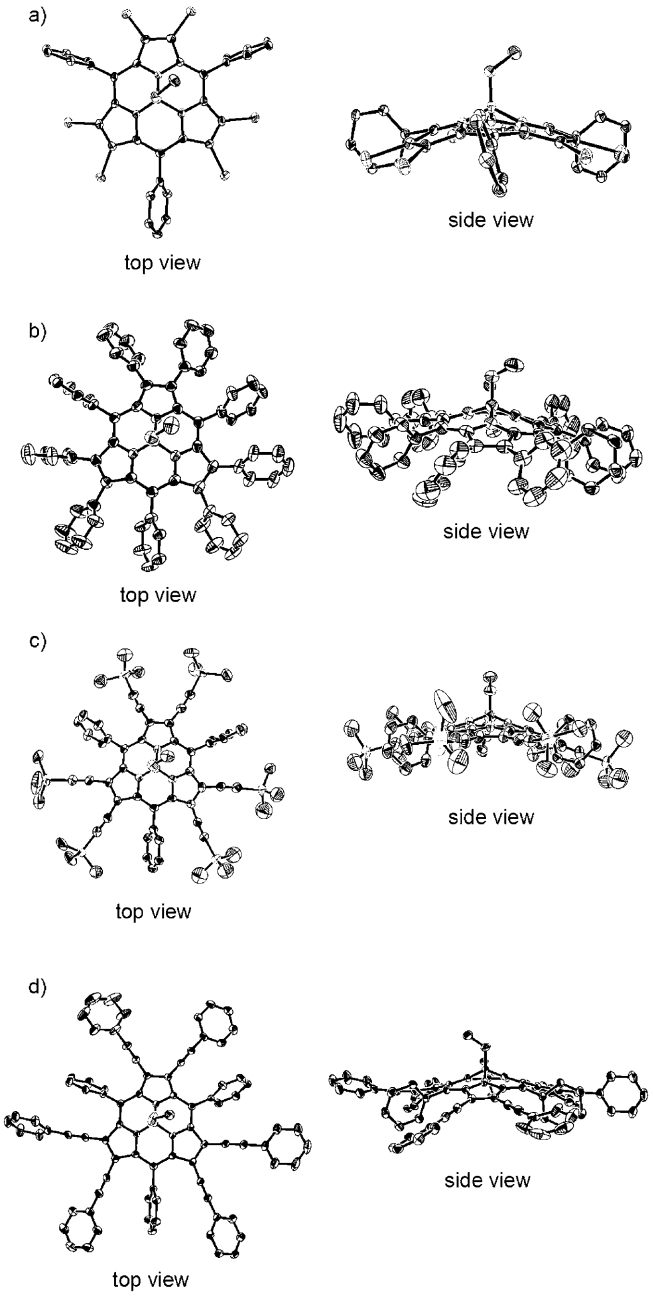

Figure 3. X-ray crystal structures of a) **2b**, b) **3b**, c) **4b**, d) **5a** at 50% probability of thermal ellipsoids. Solvent molecules and protons are omitted for clarity. *t*Bu substituents are also omitted for clarity.

Table 1. Selected structural data of subporphyrins **1b**, **2b**, **3b**, **4b**, and **5a**.

	N–B [Å]	B–O [Å]	α[a] [°]	Bowl depth[b] [Å]
1b	1.490(4), 1.500(4), 1.507(4)	1.438(4)	38.3, 45.7, 48.1	1.29
2b	1.491(6), 1.507(7), 1.489(6)	1.451(6)	75.4, 72.2, 76.3	1.24
3b	1.494(5), 1.476(6), 1.486(5)	1.453(5)	64.6, 81.9, 67.6	1.22
4b	1.509(8), 1.467(9), 1.478(9)	1.438(9)	79.5, 69.9, 71.8	1.24
5a	1.502(3), 1.502(3), 1.482(3)	1.426(3)	76.6, 76.5, 68.9	1.28

[a] Dihedral angles between *meso*-aryl ring and the plane defined by neighboring C_α-C_{meso} C_α atoms. [b] Distance from central boron atom to the mean plane of six β carbons.

are similar to those in **1b**. Dihedral angles of the *meso*-aryl substituents of **2b** are considerably larger (72.2–76.3°) than those of **1b** (38–48°), reflecting the sterically more congested situation for the former. Interestingly, these structural influences of perbromination are much smaller for *meso*-aryl-substituted subporphyrins than for *meso*-aryl-substituted porphyrins, because octabrominated tetraphenylporphyrins are known to exhibit highly nonplanar, considerably distorted saddle structures.[8–11]

Similarly, the crystal structures of **3b**, **4b**, and **5a** were determined to be all bowl-shaped structures with bowl depths of 1.22, 1.24, and 1.28 Å, respectively. Notably, there is no significant structural difference in the subporphyrin core among **2b**, **3b**, **4b**, and **5a**. B–O and B–N distances summarized in Table 1 are 1.43–1.45 and 1.47–1.51 Å, respectively, which are quite similar to those of **1**. The dihedral angles between the subporphyrin plane and the *meso*-aryl plane in **2b**, **3b**, **4b**, and **5a** are above 65°, thus notably larger than those of **1**. In addition, the dihedral angles of β-phenyl substituents of **3b** are also large, lying in the range of 65–82°. Such large dihedral angles were observed for *meso*-(2,4,6-trimethoxyphenyl)-substituted subporphyrin that exhibits restricted rotation of *meso*-aryl substituents at room temperature.[6a] Similar restricted rotations of *meso*- and β-aryl groups with large dihedral angles will be discussed later.

Variable-temperature NMR spectroscopy: One of the most attractive characteristics of *meso*-aryl-substituted subporphyrins is a remarkably large substituent effect of the *meso*-aryl group, which stems from its low rotational barrier relative to that of *meso*-tetraaryl-substituted porphyrins. In our recent publication,[6a] we revealed that *ortho*-unsubstituted *meso*-aryl substituents of subporphyrin undergo free rotation even at −90 °C in CD_2Cl_2. As described above, hexabrominated subporphyrin **2a** displays broad but split signals for the *ortho*- and *meta* protons of *meso*-phenyl substituents at $\delta = 8.10$ and 7.30 ppm (*ortho*), $\delta = 7.71$ and 7.50 ppm (*meta*) at room temperature, indicating their restricted rotation (Figure 2). At −40 °C, these broad signals became a couple of sharp doublets at $\delta = 8.14$ and 7.23 ppm (*ortho*) and a couple of triplets at $\delta = 7.74$ and 7.49 ppm (*meta*) with $J = 7.80$ Hz. On the other hand, as the temperature increased, the signals became broader and finally coalesced at 60 ± 2 °C in $CDCl_3$. The ^{1}H NMR spectrum of **2b** also showed broad and split *meso*-aryl-*ortho* peaks at $\delta = 7.83$ and 7.14 ppm, reflecting the restricted rotations of *meso*-aryl substituents. These peaks became sharp singlets at −50 °C, whereas the coalescence temperature was 115 ± 5 °C in $C_2D_2Cl_4$. The higher coalescence temperature of **2b** may be ascribed to the bulkier 3,5-di-*tert*-butylphenyl substituent. The activation barrier (ΔG_{ROT}) of the rotation of *meso*-aryl substituents in **2b** was estimated to be 67 kJ mol^{-1} by simulating temperature-dependent spectral changes of the signal due to the *ortho* protons (see Supporting Information).

In the ^{1}H NMR spectrum of **3b** at room temperature, the *ortho* protons of both the *meso*-3,5-di-*tert*-butylphenyl

groups and the β-phenyl groups were observed as split broad signals at $\delta = 7.53$ and 6.33 ppm, and $\delta = 7.15$ and 6.38 ppm, respectively, indicating the restricted rotations. Following the same procedure, the activation barrier of the rotation of the β-phenyl groups was estimated to be 69 kJ mol^{-1}. Similarly, the coalescence temperatures and ΔG_{ROT} values of hexaethynylated subporphyrins **4** and **5** were also determined and are summarized in Table 2.

Table 2. Coalescence temperatures and activation energies of rotation of *meso*-aryl substituents (ΔG_{ROT}; kJ mol^{-1}) obtained from variable-temperature 600 ^{1}H NMR studies in $CDCl_3$.

	Coalescence temperature [°C]	ΔG_{ROT} [kJ mol^{-1}]
2a	60±2	
2b	115±5[a]	67
3a	0±5	
3b	85±5[a]	69
4a	−5±2	
4b	55±5[a]	61
5a	−12±2	
5b	90±2[a]	71

[a] Measured in $C_2D_2Cl_4$.

Optical properties: Figure 4 shows the absorption and fluorescence spectra of subporphyrins **1a**–**5a** in CH_2Cl_2. As reported previously,[5,6a] subporphyrin **1a** shows a Soret-like band at 373 nm and Q-like bands at 464 and 492 nm (Table 3). Peripherally persubstituted subporphyrins **2a** and **3a** also show sharp and intense Soret-like bands at 374 and 380 nm, but the shapes of the Q-like bands are significantly altered from that of **1a**. Namely, the Q(0,0) bands are weakened and the Q(0,1) bands are intensified, similar to those of the *meso*-tris(2,4,6-trimethoxyphenyl)subporphyrin. These spectral features may suggest that the electronic interaction with the *meso*-aryl substituent is important for the shape of the Q-like bands. In line with Gouterman's four-orbital theory,[17] Time-dependent DFT calculations at the B3LYP/6–31G* levels show that the Q(0,0) band of the subporphyrin core macrocycle is a forbidden transition, whereas the Q(0,0) band of **1a** is permitted slightly through the electronic interaction with *meso*-phenyl substituents. The altered Q-like bands of **2a** and **3a** can be thus accounted for in terms of large dihedral angles of the *meso*-aryl substituents, which minimize the electronic interactions with the *meso*-aryl substituents. The Soret-like bands are considerably red-shifted for β-ethynylated subporphyrins **4a** (424 nm) and **5a** (443 nm) (Table 3). The Q-like bands are also red-shifted; 426, 506, and 533 nm for **4a** and 443, 521, and 551 nm for **5a**, but the extents of the red-shift are modest relative to those of the Soret-like bands. These red-shifts possibly originate from the effective π conjugation with β-ethynyl substituents. Notably, these conjugative interactions lead to enhancement of Q-like bands for **4a** and **5a**, similar to the trends reported for porphyrins.[9]

In contrast to the broad fluorescence spectrum of **1a**, **2a** displays the fluorescence spectrum of a vibronic structure with a low quantum yield ($\Phi_F < 0.01$, Table 3). The struc-

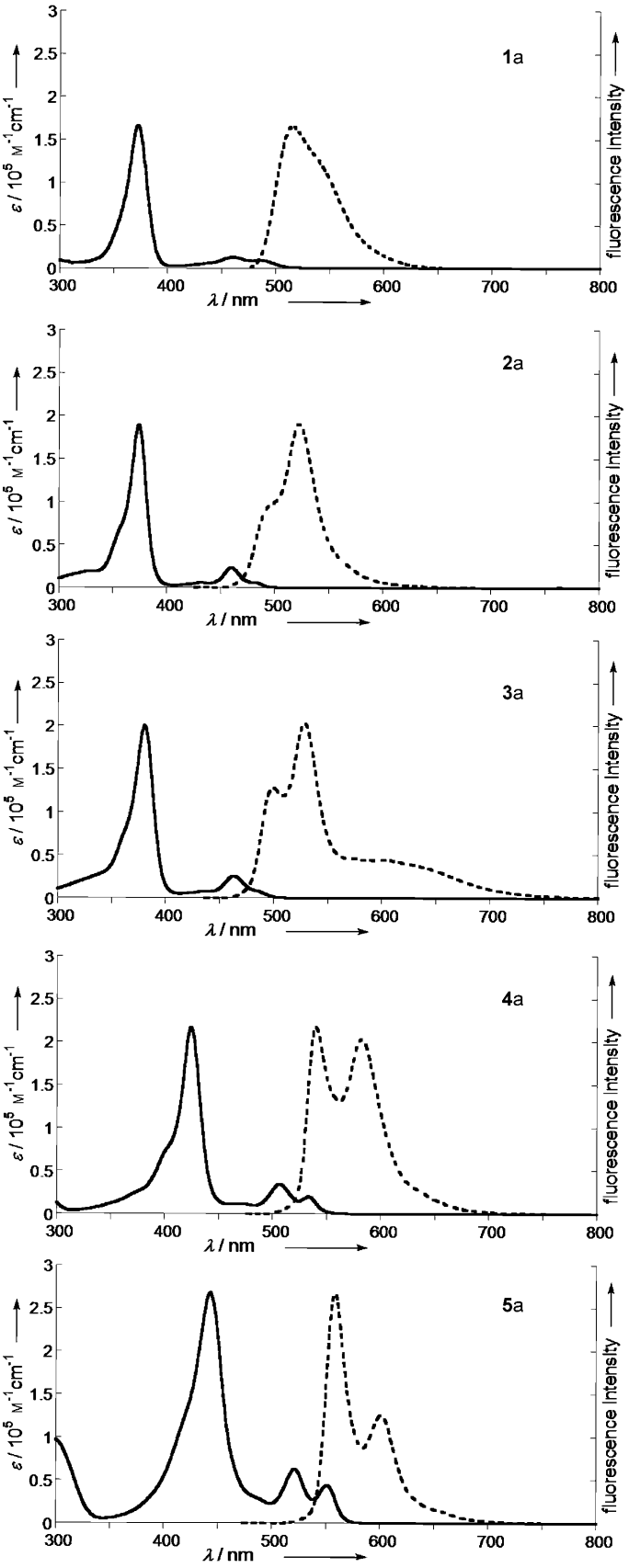

Figure 4. UV/Vis absorption (——) and emission (-----) spectra of **1a**, **2a**, **3a**, **4a**, and **5a** in CH_2Cl_2.

Table 3. Optical properties of **1**–**5** in CH_2Cl_2.

	Absorption λ [nm] (ε [10^4 M^{-1}cm^{-1}])	Fluorescence λ_{em} [nm][a]	Φ_F	τ_F[b] [ns]	σ[c] [GM]
1a	373 (16.6), 461 (1.3), 484 (0.9)	516	0.14	2.39	88
1b	373 (18.0), 464 (1.3), 492 (1.4)	524	0.11	2.83	
2a	374 (18.9), 460 (2.4)	522	<0.01	<0.01	
2b	377 (19.8), 434 (0.7), 461 (2.5)	524	<0.01		
3a	380 (20.0), 464 (2.6)	499, 528	0.12	2.58	700
3b	382 (19.9), 464 (2.7)	497, 527	0.12		
4a	424 (21.6), 506 (3.4), 533 (2.0)	540, 533	0.05	1.68	1800
4b	426 (24.2), 471 (1.2), 507 (3.8), 534 (1.8)	543 (sh), 584	0.05		
5a	443 (26.8), 521 (6.3), 551 (4.4)	558, 600	0.12	2.32	2800
5b	445 (24.1), 521(5.9), 551(3.9)	561, 603	0.12		

[a] Excited at the Soret-like band. [b] Fluorescence lifetime. [c] Two-photon-absorption cross section.

tured fluorescence can be considered also to arise from the restricted *meso*-phenyl substituent and the low fluorescence quantum yield can be ascribed to effective intramolecular heavy-atom effect. The fluorescence spectrum of **3a** also shows a vibronic structure, but with a long tail reaching over 700 nm. The fluorescence excitation spectrum of **3a** monitored at 680 nm is almost the same as its absorption spectrum (see the Supporting Information), indicating that this low-energy fluorescence is coming from the subporphyrin chromophore. The subporphyrins **4a** and **5a** exhibit distinctly red-shifted fluorescence spectra with clear vibronic structures.

The absolute fluorescence quantum yields were measured by using a closed-sphere photon-counting apparatus recorded on a Hamamatsu Photonics C9920-02 spectrometer and the observed results are summarized in Table 3. Whereas the fluorescence quantum yields of **3a** and **5a** (both cases; $\Phi_F = 0.12$) are similar to that of **1a** ($\Phi_F = 0.14$), those of **2a** and **4a** are significantly smaller; $\Phi_F < 0.01$ and 0.05, respectively. The observed low fluorescence quantum yield of **2a** is apparently due to the efficient intramolecular heavy-atom effect, whereas the reason for the low quantum yield of **4a** is unclear. The fluorescence lifetimes were measured by the single-photon counting system, by exciting at 424 nm. The fluorescence lifetimes of **3a** (2.58 ns) and **5a** (2.32 ns) are very close to that of **1a** (2.39 ns), whereas that of **4a** is slightly shorter (1.68 ns).

The electronic effects of peripheral substituents on the subporphyrin ring is examined further from two-photon-absorption (TPA) cross-section ($\sigma^{(2)}$) values, which are largely proportional to the electron-delocalization strength of the molecule.[18] The TPA cross-section values were obtained from the open aperture Z-scan traces, as shown in Figure 5, by exciting the molecule at 800 nm with 130 fs optical pulses.[19,20] The TPA cross-section values of **1a**, **3a**, **4a**, and **5a** were measured to be 88,[9d] 700, 1800, and 280 GM (1 GM = 10^{-50} cm^4 s/photon/molecule), respectively (Table 3). These results indicate that β-ethynyl substituents in **4a** and **5a** are quite effective for the enhancement of TPA values by virtue of enhanced electron delocalization. Notably, the TPA cross-section value of **5a** is about four times larger than that of its *meso* (*meso*-tris(4-phenylacetylene)subporphyrin)-substituted counterpart (660 GM),[9d] due to the direct ethyne linkage to the subporphyrin core, whereas the phenyl ring acts as a bridge for the latter. Although direct ethyne linkage ensures efficient electron delocalization, the phenyl group, which remains nearly orthogonal with the subporphyrin ring, precludes the effective π conjugation. In addition, as the number of π-electron-communicated branches is one of the

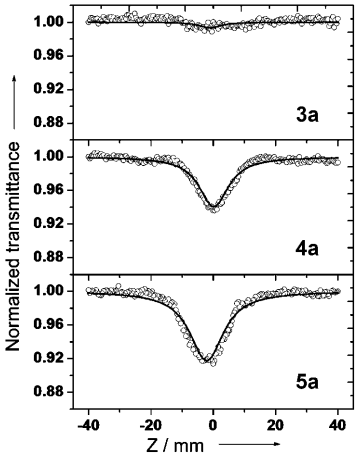

Figure 5. The open aperture Z-scan traces of **3a** (top), **4a** (middle), and **5a** (bottom). The solid lines are the best-fitted curves of experimental data.

crucial factors for the TPA properties of molecules,[21] it is significant that six aryl substituents at β positions contrast with three at *meso* positions. Another important contributing aspect for the observed larger TPA cross-section value could be the octupolar structure of subporphyrin with threefold symmetry.[9d,22] The octupolar compounds are known to exhibit larger first-order hyperpolarizabilities than their dipolar counterparts. These hyperpolarizabilities were found to show approximately a linear relationship with two-photon-absorption capabilities, and both values increase monotonically as the π-conjugation length increases.[22a] Thus, the enhanced TPA properties of subporphyrins are accounted for in terms of both electron-delocalization strength and octupolar effect. Indeed, the octupolar effect contributed by the increased π-conjugation pathway seems to be larger than the actual π-conjugation effect, as demonstrated by the considerably higher TPA cross-section values of **5a** relative to **4a**.

Electrochemical properties and DFT calculations: The oxidation and reduction potentials of substituted subporphyrins **1b**–**5b** were measured by cyclic voltammetry in CH_2Cl_2 versus the ferrocene/ferrocenium ion couple to examine the

influence of β substituents on the electronic property of subporphyrins (Table 4). Subporphyrins **1b**, **2b**, and **3b** exhibit the first-oxidation and -reduction potentials as reversible waves at 0.78 and −1.82 V, 1.10 and −1.71 V, and 0.64 and −2.12 V, respectively, hence allowing the estimation of the electrochemical HOMO–LUMO gap to be 2.60, 2.81, and 2.76 eV, respectively. The observed β-substituent effects are analogous to those of Ni^{II}-TPP[10] with respect to potential shift (higher for bromo and lower for phenyl; Table 4), but differ substantially with respect to the electrochemical HOMO–LUMO gap. For Ni^{II}-TPP, the HOMO–LUMO gap distinctly decreases in the order of unsubstituted > octaphenylated > octabrominated, whereas the order of subporphyrins is just the opposite. The trend for observed Ni^{II}-TPP can be explained as follows: the electrochemical potentials are shifted linearly to intrinsic substituent effect, however, conformations of octabrominated and octaphenylated porphyrins are significantly distorted, which lifts up the HOMO level depending upon steric congestion due to β substituents. On the other hand, such steric congesting effects are not serious for subporphyrin macrocycles, as indicated by the similar solid-state structures for **1b**, **2b**, **3b**, **4b**, and **5a**. Therefore, the inductive effects of β substituents are dominant for the electrochemical potentials of β-substituted subporphyrins. This minor influence of the steric effects for subporphyrins stems apparently from more spatial room for β substituents.

Table 4. Oxidation and reduction potentials [V vs ferrocene/ferrocenium ion pair].[a]

	$E^1_{1/2,ox}$	$E^1_{1/2,red}$	HOMO–LUMO gap
1b	0.78	−1.82	2.60
2b	1.10	−1.71	2.81
3b	0.64	−2.12	2.76
4b	0.87	−1.65	2.52
5b	0.83	−1.58	2.41
Ni(TPP)[b]	1.05	−1.28	2.33
$Ni(Br_8TPP)$[b]	1.20	−0.80	2.00
Ni(DPP)[b]	0.75	−1.37	2.12

[a] Measured by cyclic voltammetry using a glassy-carbon working electrode, a platinum-wire counter electrode, and Ag/0.01 M $AgClO_4$ reference electrode. The measurements were recorded in CH_2Cl_2 solutions containing 0.10 M Bu_4NPF_6 as a supporting electrolyte. [b] See ref. [10]; TPP = tetraphenylporphyrin, DPP = dodecaphenylporphyrin.

Hexaethynylated analogues **4b** and **5b** exhibit the first-reduction and -oxidation potentials at −1.65 and 0.87 V, and −1.58 and 0.83 V, respectively, which correspond to decreased electrochemical HOMO–LUMO gaps of 2.52 and 2.41 V, respectively, probably as a consequence of the extension of π-conjugation networks. These data are nicely in line with the optical HOMO–LUMO gaps, 2.32 and 2.25 eV for **4b** and **5b** in CH_2Cl_2, respectively.

Molecular orbital (MO) calculations were performed at the B3LYP/6–31G* levels with the Gaussian 03 package[23] (Figure 6 and Table 4). We have previously reported that *meso*-aryl-substituted subporphyrins possess quite porphyrin-like four orbitals, HOMO-1 (a_2), HOMO (a_1), LUMO (e), and LUMO+1 (e), and that their HOMO, LUMO, and LUMO+1 characteristically show large electronic coefficients on *meso*-aryl substituents, explaining the large influences of *meso*-aryl rings on their electronic properties. As shown in Figure 6, MO diagrams of β-substituted subporphyrins **2a** and **3a** exhibit similar porphyrin-like four orbitals, but small electronic coefficients on *meso*-aryl rings due to their large dihedral angles, similar to *meso*-2,4,6-trimethoxyphenyl-substituted subporphyrin.[6a] Calculated MO diagrams also show stabilized HOMO and LUMO of **2a**, destabilized HOMO and LUMO of **3a**, and increments of HOMO–LUMO gaps of **2a** and **3a**, which are all consistent with the experimental results.

The MO diagrams of **5a** exhibit significantly stabilized LUMO and slightly destabilized HOMO, leading to the decrease of the HOMO–LUMO gap. In addition, anti-phase hybridization of ethynes at β positions resulted in the remarkable destabilization of a_2 orbital, which causes the decrease in the energy gap between a_1 and a_2 orbitals. These interactions gave rise to the substantial bathochromic shift of the Soret-like band. Briefly, these β-substituted subporphyrins are still explainable within Gouterman's four-orbital theory. The four orbitals of **5a** show large coefficients on their terminal phenyl rings through ethyne bonds, which indicates the possibility for further introductions of substituents to the terminal phenyl rings.

Conclusion

Suzuki–Miyaura and Stille coupling reactions were effectively performed for β-perbrominated subporphyrin substrates as the first fabrication reactions at the periphery. These results demonstrate that the peripheral-substitution reactions of porphyrins are similarly useful for subporphyrins, which will allow further functionalizations of subporphyrins. Interestingly, however, the influences of these per-fabrications at the periphery are quite different between porphyrin and subporphyrin. Whereas the structural distortions are dominant for the former, such effects are only small or modest for the latter. The substituent effects at the β position of subporphyrins on the optical and electronic properties are explained in terms of Gourterman's four-orbital theory, despite their C_3 symmetry. Furthermore, nonlinear optical properties of these subporphyrins are predominantly due to the octupolar effect instead of increased π-conjugation length. Synthetic studies along this line are worthy of further investigation, and are actively in progress in our laboratory.

Experimental Section

General: Dry pyrrole was distilled from CaH_2. Pyridine used for the preparation of PPB was dried over activated molecular sieves 4A. Borane-triethylamine complex was purchased from Aldrich and used as received. Dry THF and toluene were obtained from Wako Inc., and other reagents and solvents were of commercial-reagent grade and were used without further purification. ^1H, ^{11}B, and ^{13}C NMR spectra were re-

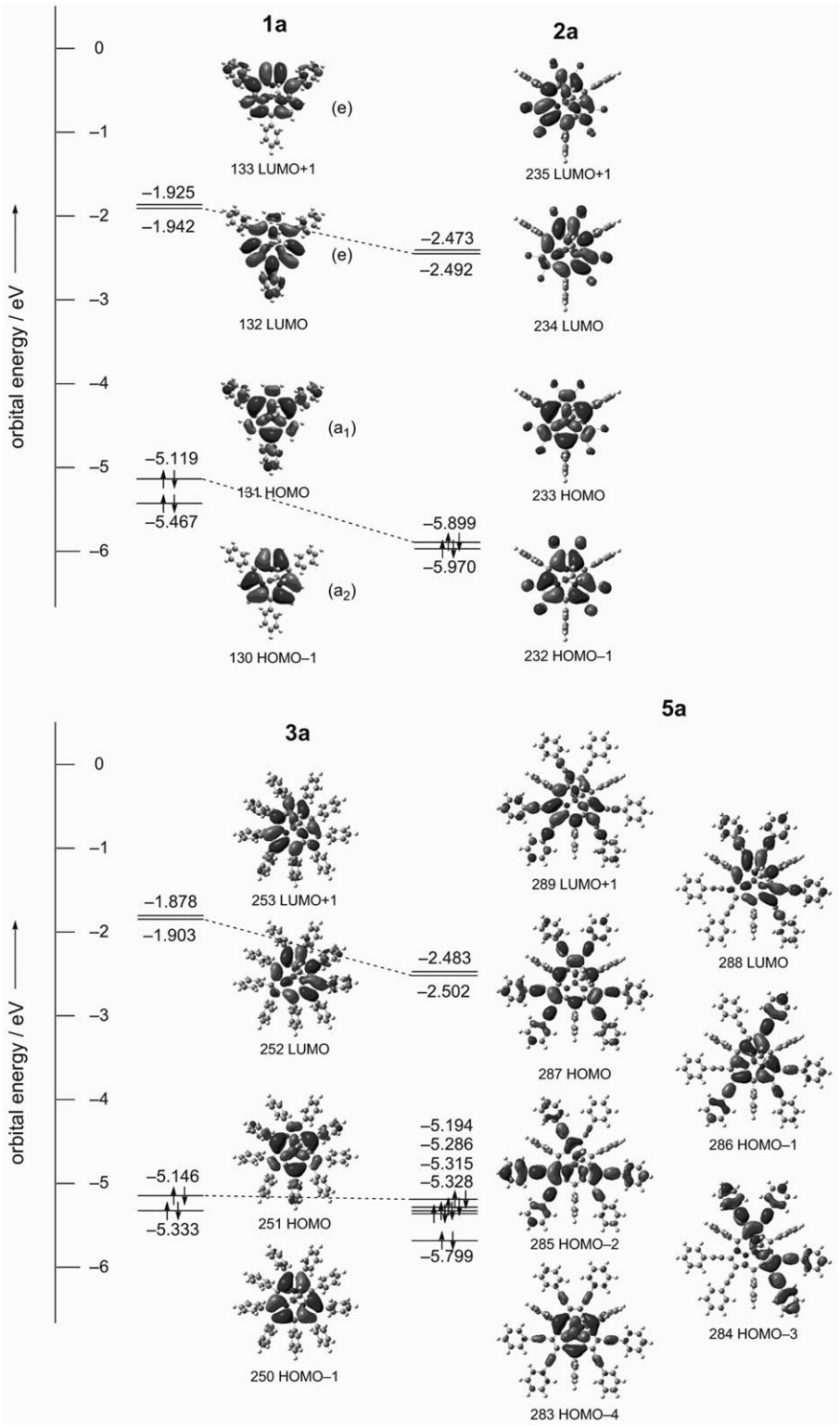

Figure 6. Molecular orbital diagrams of **1a** (top, left), **2a** (top, right), **3a** (bottom, left), and **5a** (bottom, right) calculated at the B3LYP/6-31G* levels.

corded by using a JEOL delta-600 spectrometer, and chemical shifts were reported as the delta scale in ppm relative to internal standards ($CHCl_3$ ($\delta = 7.26$ ppm for ^1H, 77.16 ppm for ^{13}C), $C_2H_2Cl_4$ ($\delta = 5.98$ ppm for ^1H), and an external standard, $BF_3{\cdot}OEt_2$ in $CDCl_3$ ($\delta = 0.00$ ppm for ^{11}B). Spectroscopic-grade solvents were used for all spectroscopic studies without further purification. UV/Vis absorption spectra were recorded by using a Shimadzu UV-3100 spectrometer. Fluorescence spectra were recorded by using a Hamamatsu Photonics C9920–02 spectrometer, and absolute fluorescence quantum yields were measured by the photon-counting method using the same model with an integration sphere. ESI-TOF mass spectra were recorded by using a Bruker Dalronics micro TOF LC using positive-ion mode. MALDI-TOF mass spectra were recorded by using a Shimadzu/Kratos Kompact MALDI 4 spectrometer using the positive-MALDI ionization method. Redox potentials were measured by cyclic voltammetry using an ALS electrochemical analyzer model 660. Preparative separations were achieved by performing silica-gel chromatography (GPC) (Bio-Rad Bio-Beads S-X1, packed with THF in a 4×80-cm gravity column).

Pyridine-tri-*N*-pyrrolylborane (PPB): Borane-triethylamine complex (42.7 mL, 0.288 mol) and freshly distilled pyrrole (60 mL, 0.865 mol) were added by using a syringe to a carefully dried 300-mL round-bottomed flask equipped with N_2 inlet–outlet and distillation head. The mixture was heated to 100 °C for 2.5 h in an oil bath under N_2, and then the bath temperature was elevated to 160 °C. The triethylamine generated was distilled off to leave a pale yellow cake. Once the solidification was confirmed, the flask was removed immediately from the oil bath. The crude tri-*N*-pyrrolylborane thus obtained was dried in vacuo below 100 °C, then the flask was refilled with dry N_2. Dry pyridine (225 mL) was added to the solid and heated to 100 °C, and the resulting suspension was vigorously stirred. When the solid material was completely dissolved, heating was stopped and the clear solution was slowly cooled to 0 °C to leave colorless crystals. The precipitation was filtered and washed with a minimal amount of cold hexane, then dried in vacuo to give 53 g of pyridine-*N*-tripyrrolylborane (PPB) in 64% yield as a colorless, crystalline solid. ^1H NMR (600 MHz, $CDCl_3$): $\delta = 8.14$ (t, $J = 7.3$ Hz, 1H; pyridine-*p*-H), 8.10 (br, 2H; pyridine-*o*-H), 7.63 (t, $J = 6.9$ Hz, 2H; pyridine-*m*-H), 6.63 (dd, $J = 2.3$, 1.9 Hz, 6H; pyrrole), 6.27 ppm (dd, $J = 2.3$, 1.9 Hz, 6H; pyrrole); ^{11}B NMR (193 MHz, $CDCl_3$): $\delta = 4.1$ ppm (s, 1B); ^{13}C NMR (150 MHz, $CDCl_3$): $\delta = 146.2$ (pyridine-*o*), 142.7 (pyridine-*p*), 125.9 (pyridine-*m*), 124.2 (pyrrole), 109.8 ppm (pyrrole).

Methoxo(2,3,7,8,12,13-hexabromo-5,10,15-triphenylsubporphyrinate)boron(III) (2a): Bromine (0.1 mL) was added to a solution of

1a (24.3 mg, 48.4 μmol) in deoxygenated $CHCl_3$ (20 mL) in a 50-mL round-bottomed flask, and the resulting solution was stirred at room temperature for 2 h under N_2 atmosphere. The reaction was quenched by the addition of saturated $Na_2S_2O_3$ solution (10 mL) and then the organic layer was separated and washed with water twice and brine, dried over anhydrous Na_2SO_4, and concentrated in vacuo. A mixture of CH_2Cl_2/MeOH (1:1, 20 ml) was added to the residue, and heated at 50 °C for 10 min followed by concentration in vacuo. The crude material was purified by short path on silica with CH_2Cl_2/hexane/ether = 1:4:1 as an eluent and recrystallization from CH_2Cl_2/MeOH gave pure subporphyrin **2a** (46.4 mg, quant.) as a yellow solid. ^{1}H NMR (600 MHz, $CDCl_3$, −40 °C): δ = 8.12 (d, J = 7.80 Hz, 3H; *meso*-Ph-*ortho*), 7.74 (t, J = 7.80 Hz, 3H; *meso*-Ph-*meta*), 7.69 (t, J = 7.80 Hz, 3H; *meso*-Ph-*para*), 7.49 (t, J = 7.80 Hz, 3H; *meso*-Ph-*meta*), 7.23 (d, J = 7.80 Hz, 3H; *meso*-Ph-*ortho*), 0.84 ppm (s, 3H; axial-OMe); ^{11}B NMR (193 MHz, $CDCl_3$, −40 °C): δ = −16.2 ppm (s); ^{13}C NMR (150 MHz, $CDCl_3$, RT): δ = 135.1, 133.3, 132.6, 132.3, 129.4, 127.9, 120.1, 118.1, 47.4 ppm; UV/Vis (CH_2Cl_2): λ_{max} (ε) = 374 (189000), 460 nm (24000 $M^{-1}cm^{-1}$); fluorescence (CH_2Cl_2, λ_{ex} = 374 nm): λ_{max} = 522 nm; Φ_F < 0.01; HR-ESI TOF-MS (positive mode): m/z: calcd for $C_{33}H_{15}N_3B_1Br_6$: 943.6402 $[M-OMe]^+$; found: 943.6395.

Methoxo(2,3,7,8,12,13-hexabromo-5,10,15-tri(3,5-di-*tert*-butylphenyl)-subporphyrinate)boron(III) (2b): The subporphyrin **2b** was prepared from **1b** (18.6 mg, 22.2 μmol) by the same procedure used for the preparation of **2a**. Yield was 24.9 mg (88%). A single crystal suitable for X-ray diffraction analysis was prepared by slow recrystallization from CH_2Cl_2/MeOH. ^{1}H NMR (600 MHz, $CDCl_3$, RT): δ = 7.83 (s, 3H; *meso*-Ar-*ortho*), 7.62 (s, 3H; *meso*-Ar-*para*), 7.14 (s, 3H; *meso*-Ar-*ortho*), 1.47 (s, 27H; *meso*-Ar-*tert*-butyl), 1.29 (s, 27H; *meso*-Ar-*tert*-butyl), 0.86 ppm (s, 3H; axial-methoxy); ^{11}B NMR (193 MHz, $CDCl_3$, RT): δ = −16.1 ppm; ^{13}C NMR (151 MHz, $CDCl_3$, RT): δ = 150.4, 149.5, 134.5, 131.1, 128.3, 127.4, 122.3, 121.1, 118.0, 47.5, 35.3, 35.2, 31.8, 31.6 ppm; UV/Vis (CH_2Cl_2): λ_{max} (ε) = 377 (198000), 434 (7000), 461 nm (25000 $M^{-1}cm^{-1}$); fluorescence (CH_2Cl_2, λ_{ex} = 374 nm): λ_{max} = 524 nm; Φ_F < 0.01; HR-ESI TOF-MS (positive mode): m/z: calcd. for $C_{57}H_{63}N_3B_1Br_6$: 1280.0179 $[M-OMe]^+$; found: 1280.0181.

Methoxo(2,3,5,7,8,10,12,13,15-nonaphenylsubporphyrinate)boron(III) (3a): A sample test tube containing **2a** (28.3 mg, 30.2 μmol), dihydroxyphenylboron (110.0 mg, 898 μmol), and $CsCO_3$ (675.4 mg, 2.07 mmol) was purged with N_2, and then charged with dehydrated toluene (6 mL). [Pd(PPh_3)$_4$] (20.1 mg, 17.5 μmol) was added to the mixture and stirred at 110 °C for four days under N_2 conditions. The resulting solution was cooled to room temperature, diluted with 10 mL of CH_2Cl_2, washed with water twice, dried over anhydrous Na_2SO_4, and then concentrated in vacuo. A mixture of CH_2Cl_2/MeOH (1:1, 20 mL) was added to the residue and heated at 50 °C for 10 min followed by concentration in vacuo. The resulting mixture was concentrated in vacuo and then purified by column chromatography on silica with CH_2Cl_2/hexane/diethyl ether = 1:4:1 as an eluent. The ^{1}H NMR spectrum of the mixture indicated the presence of β-pentaphenylated product. Repeated silica-gel column chromatography and recrystallization from CH_2Cl_2/MeOH gave pure **3a** as a yellow solid. As a more convenient method, one more cycle of bromination with bromine and subsequent Suzuki–Miyaura coupling reaction of the mixture of β-pentaphenylated product and **3a** gave pure **3a** in 55% yield without difficult separation. ^{1}H NMR (600 MHz, $CDCl_3$, −50 °C): δ = 7.29 (d, J = 7.32 Hz, 3H; *meso*-Ph-*ortho*), 6.89 (d, J = 7.32 Hz, 6H; β-Ph-*ortho*), 6.80 (t, J = 7.74 Hz, 3H; *meso*-Ph-*para*), 6.78 (t, J = 6.90 Hz, 6H; β-Ph-*para*), 6.72 (t, J = 7.32 Hz, 6H; β-Ph-*meta*), 6.59 (t, J = 8.22 Hz, 3H; *meso*-Ph-*meta*), 6.27 (br, 6H; β-Ph-*meta*), 6.24 (t, 8.22 Hz, 3H; *meso*-Ph-*meta*), 6.09 (d, J = 6.90 Hz, 3H; *meso*-Ph-*ortho*), 6.05 (d, J = 6.00 Hz, 6H; β-Ph-*ortho*), 0.70 ppm (s, 3H; axial-OMe); ^{11}B- and ^{13}C NMR spectra were not recorded because of poor solubility. UV/Vis (CH_2Cl_2): λ_{max} (ε) = 380 (200000), 464 nm (26000 $M^{-1}cm^{-1}$); fluorescence (CH_2Cl_2, λ_{ex} = 374 nm): λ_{max} = 499, 528 nm; Φ_F = 0.12; HR-ESI TOF-MS (positive mode): m/z: calcd for $C_{69}H_{45}N_3B_1$: 926.3712 $[M-OMe]^+$; found: 926.3710.

Methoxo(2,3,7,8,12,13-hexaphenyl-5,10,15-tri(3,5-di-*tert*-butylphenyl)-subporphyrinate)boron(III) (3b): The subporphyrin **3b** was prepared from **2a** (25.1 mg, 19.6 μmol) by the same procedure used for the preparation of **3a**. Yield was 18.4 mg (73%). A single crystal suitable for X-ray diffraction analysis was prepared by slow recrystallization from CH_2Cl_2/methanol. ^{1}H NMR (600 MHz, $CDCl_3$, −50 °C): δ = 7.53 (s, 3H; *meso*-Ar-*ortho*), 7.15 (d, J = 7.32 Hz, 6H; β-Ph-*ortho*), 6.8–6.9 (m, 9H; *meso*-Ar-*para*, β-Ph-*para*), 6.80 (t, J = 7.32 Hz, 6H; β-Ph-*meta*), 6.63 (t, J = 7.32 Hz, 6H; β-Ph-*meta*), 7.53 (d, J = 7.32 Hz, 6H; β-Ph-*ortho*), 6.33 (s, 3H; *meso*-Ar-*ortho*), 1.09 (s, 27H; *meso*-Ar-*tert*-butyl), 0.83 (s, 27H; *meso*-Ar-*tert*-butyl), 0.81 ppm (s, 3H; axial-OMe); ^{11}B NMR (193 MHz, $CDCl_3$, −50 °C): δ = −15.5 ppm; ^{13}C NMR (150 MHz, $CDCl_3$, −50 °C): δ = 147.8, 147.3, 138.3, 136.6, 134.7, 133.6, 132.0, 130.3, 127.7, 126.7, 126.4, 126.3, 125.5, 122.3, 121.7, 47.5, 34.4, 34.1, 31.4, 31.1 ppm; UV/Vis (CH_2Cl_2): λ_{max} (ε) = 382 (199000), 464 nm (27000 $M^{-1}cm^{-1}$); fluorescence (CH_2Cl_2, λ_{ex} = 374 nm): λ_{max} = 497, 522 nm; Φ_F = 0.12; HR-ESI TOF-MS (positive mode): m/z: calcd for $C_{93}H_{93}N_3B_1$: 1262.7471 $[M-OMe]^+$; found: 1262.7470.

Methoxo(2,3,7,8,12,13-hexa(trimethylsilylethynyl)-5,10,15-phenyl)-subporphyrinate)boron(III) (4a): A sample test tube containing **2a** (47.3 mg, 50.4 μmol) was purged with N_2, and then charged with dry THF (10 mL). [Pd(PPh_3)$_4$] (37.0 mg, 32.1 μmol) and tributyl(trimethylsilylethynyl)tin(III) (189.5 mg, 489.3 μmol) was added to the mixture and the resulting solution was stirred at 70 °C for 24 h under N_2 atmosphere. The resulting mixture was cooled to room room temperature, washed with water twice, dried over anhydrous Na_2SO_4, and then concentrated in vacuo. A mixture of CH_2Cl_2/MeOH (1:1) was added to the residue and heated at 50 °C for 10 min followed by concentration in vacuo. The crude material was purified by a short silica-gel column using a mixture of CH_2Cl_2/hexane/diethyl ether = 1:4:1 as an eluent. Recrystallization from CH_2Cl_2/MeOH gave pure subporphyrin **4a** (46.1 mg, 85%) as a red solid. ^{1}H NMR (600 MHz, $CDCl_3$, RT): δ = 7.72 (br, 6H; *meso*-Ph-*ortho*), 7.59 (t, 3H; J = 7.80 Hz, *meso*-Ph-*para*), 7.49 (t, J = 7.32 Hz, 6H; *meso*-Ph-*meta*), 0.90 (s, 3H; axial-OMe), 0.11 ppm (s, 54H; β-TMS); ^{11}B NMR (193 MHz, $CDCl_3$, RT): δ = −15.4 ppm; ^{13}C NMR (150 MHz, $CDCl_3$, RT): δ = 138.6, 133.8, 133.2, 129.0, 127.3, 123.9, 120.2, 108.2, 97.3, 47.2, 0.23 ppm; UV/Vis (CH_2Cl_2): λ_{max} (ε) = 424 (216000), 506 (34000), 533 nm (20000 $M^{-1}cm^{-1}$); fluorescence (CH_2Cl_2, λ_{ex} = 424 nm): λ_{max} = 540, 583 nm; Φ_F = 0.05; HR-ESI TOF-MS (positive mode): m/z: calcd for $C_{63}H_{69}N_3B_1Si_6$: 1046.4206 $[M-OMe]^+$; found: 1046.4206.

Methoxo(2,3,7,8,12,13-hexa(trimethylsilylethynyl)-5,10,15-tri(3,5-di-*tert*-butylphenyl)subporphyrinate)boron(III) (4b): The subporphyrin **4b** was prepared from **2b** (37.5 mg, 29.3 μmol) by the same procedure used for the preparation of **4a** except the reaction temperature was 110 °C. Yield was 18.5 mg (63%). A single crystal suitable for X-ray diffraction analysis was prepared by slow recrystallization from CH_2Cl_2/methanol. ^{1}H NMR (600 MHz, $CDCl_3$, −50 °C): δ = 7.93 (s, 3H; *meso*-Ar-*ortho*), 7.54 (s, 3H; *meso*-Ar-*para*), 6.96 (s, 3H; *meso*-Ar-*ortho*), 1.46 (s, 27H; *meso*-Ar-*tert*-butyl), 1.27 (s, 27H; *meso*-Ar-*tert*-butyl), 0.92 ppm (s, 3H; axial-OMe); ^{11}B NMR (193 MHz, $CDCl_3$, RT): δ = −15.6 ppm (s); ^{13}C NMR (150 MHz, $C_2D_2Cl_4$, 100 °C): δ = 148.8, 137.2, 133.5, 127.7, 125.7, 121.8, 120.6, 108.3, 98.3, 47.6, 35.0, 32.0, 0.9 ppm; UV/Vis (CH_2Cl_2): λ_{max} (ε) = 426 (242000), 471 (12000), 507 (38000), 534 nm (18000 $M^{-1}cm^{-1}$); fluorescence (CH_2Cl_2, λ_{ex} = 426 nm): λ_{max} = 543 (sh), 584 nm; Φ_F = 0.05; HR-ESI TOF-MS (positive mode): m/z: calcd for $C_{87}H_{117}N_3B_1Si_6$: 1383.7982 $[M-OMe]^+$; found: 1383.7987.

Methoxo(2,3,7,8,12,13-hexa(phenylethynyl)-5,10,15-phenyl)subporphyrinate)boron(III) (5a): A sample test tube containing **2a** (27.8 mg, 29.6 μmol) and trimethyl(phenylethynyl)tin(III) (60.0 mg, 240 μmol) was purged with N_2, and then charged with dehydrated THF (6 mL). [Pd(PPh_3)$_4$] (23.1 mg, 20.1 μmol) was added to the mixture and the resulting solution was stirred at 70 °C for 24 h under N_2 atmosphere. The resulting mixture was cooled to RT, washed with water twice, dried over anhydrous Na_2SO_4, and then concentrated in vacuo. A mixture of CH_2Cl_2/MeOH (1:1) was added to the residue and heated at 50 °C for 10 min followed by concentration in vacuo. The crude material was purified with a short silica-gel column using a mixture of CH_2Cl_2/hexane/diethyl ether = 1:4:1 as an eluent. Recrystallization from CH_2Cl_2/MeOH gave pure subporphyrin **5a** (26.4 mg, 89% yield) as a red solid. A single crystal suitable for X-ray diffraction analysis was prepared by slow recrystallization from CH_2Cl_2/methanol. ^{1}H NMR (600 MHz, $CDCl_3$, −60 °C): δ = 8.43 (br, 3H;

Table 5. Crystal data and structure refinement for **2b**, **3b**, **4b**, and **5b**.

	PPB	**2b**	**3b**	**4b**	**5a**
formula	$C_{17}H_{17}BN_4$	$C_{60}H_{69}BN_3O_3Br_6$	$C_{94}H_{96}BN_3O$	$C_{88}H_{120}BN_3OSi_6$	$C_{82}H_{48}BN_3O$
crystal size [mm]	0.60×0.50×0.40	0.20×0.15×0.10	0.50×0.25×0.15	0.70×0.25×0.10	0.40×0.25×0.20
color	colorless	yellow	yellow	red	red
formula weight	288.16	1370.45	1294.62	1517.18	1102.04
crystal system	triclinic	monoclinic	triclinic	monoclinic	triclinic
space group	$P\bar{1}$	$P2_1/c$	$P\bar{1}$	Cc	$P\bar{1}$
a [pm]	8.401(5)	16.722(2)	16.397(6)	17.311(4)	12.585(4)
b [pm]	10.150(7)	9.1399(10)	16.687(5)	32.850(7)	14.470(5)
c [pm]	10.264(7)	39.858(5)	17.383(5)	18.949(5)	19.038(6)
α [°]	60.76(3)	90	100.410(8)	90	109.040(12)
β [°]	83.37(2)	95.456(6)	90.246(11)	113.281(8)	92.545(12)
γ [°]	80.39(3)	90	110.725(11)	90	114.667(10)
V [nm^3]	0.7524(9)	6.0641(13)	4.363(2)	9.899(4)	2911.7(16)
Z	2	4	2	4	2
T [K]	123(2)	123(2)	123(2)	123(2)	123(2)
ρ_{calcd} [mg m^{-3}]	1.272	1.501	0.985	1.018	1.257
$2\theta_{max}$ [°]	54.92	54.92	50	50	54.92
total reflns	7435	53572	34074	38757	28733
unique reflns	3415	13822	15249	16264	12870
reflns obs. [$I>2\sigma(I)$]	2860	10108	7425	9681	8484
parameters	199	13822	973	1050	796
restraints	0	677	878	732	38
μ [mm^{-1}]	0.077	4.017	0.057	0.179	0.074
R_1 [$I>2\sigma(I)$]	0.0467	0.0543	0.0987	0.0926	0.0599
wR_2 (all data)	0.0383	0.1436	0.3064	0.2750	0.1990
GOF on F^2	1.109	1.034	1.004	0.991	1.034
residual density [e Å^{-3}]	0.245 / −0.214	2.174 / −0.836	1.211 / −0.604	0.791 / −0.475	0.626 / −0.689

meso-Ar-*ortho*), 7.87 (br, 3H; *meso*-Ar-*meta*), 7.78 (t, $J=7.56$ Hz, 3H; *meso*-Ar-*para*), 7.55 (br, 3H; *meso*-Ar-*ortho*), 7.51 (br, 3H; *meso*-Ar-*meta*), 7.37–7.31 (m, 18H; β-Ph-*meta*, β-Ph-*para*), 7.25 (br, 12H; β-Ph-*ortho*), 1.19 ppm (s, 3H; axial-methoxy); ^{11}B NMR (193 MHz, $CDCl_3$, −60 °C): $\delta=-15.3$ ppm (s); ^{13}C NMR (151 MHz, $CDCl_3$, −60 °C): $\delta=$ 137.9, 133.4, 133.3, 131.9, 129.1, 128.6, 128.2, 127.7, 127.4, 122.8, 122.7, 119.5, 102.0, 95.9, 83.7, 51.3 ppm; UV/Vis (CH_2Cl_2): λ_{max} (ε) = 443 (268000), 521 (63000), 551 nm (44000 M^{-1}cm^{-1}); fluorescence (CH_2Cl_2, $\lambda_{ex}=445$ nm): $\lambda_{max}=561$ nm; $\Phi_F=0.11$; HR-ESI TOF-MS (positive mode): m/z: calcd for $C_{93}H_{93}N_3B_1$: 1262.7471 [M−OMe]$^+$; found: 1262.7470.

Methoxo(2,3,7,8,12,13-hexa(phenylethynyl)-5,10,15-tri(3,5-di-*tert*-butylphenyl)subporphyrinate)boron(III) (5b): The subporphyrin **5b** was prepared from **2b** (25.1 mg, 19.6 μmol) by the same procedure used for the preparation of **5a** except the reaction temperature was 110 °C. Yield was 21.0 mg (74%). ^{1}H NMR (600 MHz, $CDCl_3$, −40 °C): $\delta=8.27$ (s, 3H; *meso*-Ar-*ortho*), 7.74 (s, 3H; *meso*-Ar-*para*), 7.32–7.26 (m, 18H; β-Ph-*meta*, β-Ph-*para*), 7.21 (s, 3H; *meso*-Ar-*ortho*), 7.16 (d, $J=6.42$ Hz, 12H; β-Ph-*ortho*), 1.19 ppm (s, 3H; axial-methoxy); ^{11}B NMR (193 MHz, $CDCl_3$, −60 °C): $\delta=-14.9$ ppm (s); ^{13}C NMR (125 MHz, $CDCl_3$, −60 °C): $\delta=$ 148.6, 148.5, 138.7, 133.0, 128.5, 128.3, 127.9, 127.2, 122.7, 122.5, 120.8, 102.0, 95.9, 83.6, 47.4, 35.1, 34.6, 31.7, 31.1 ppm; UV/Vis (CH_2Cl_2): λ_{max} (ε) = 445 (241000), 521 (59000), 551 nm (39000 M^{-1}cm^{-1}); fluorescence (CH_2Cl_2, $\lambda_{ex}=445$ nm): $\lambda_{max}=561$, 603 nm; $\Phi_F=0.10$; HR-ESI TOF-MS (positive mode): m/z: calcd for $C_{105}H_{93}N_3B_1$: 1407.7499 [M−OMe]$^+$; found: 1407.7499.

Crystallographic data: X-ray data were recorded by using a Rigaku–Raxis imaging-plate system. The structures were solved by direct methods (Sir 97[24] or SHELXS-97[25]). Structure refinement was carried out by using SHELXL97.[25] Table 5 lists crystallographic details.

CCDC-699898 (**2b**), CCDC-699899 (**3b**), CCDC-699900 (**4b**), CCDC-699901 (**5a**), and CCDC-699902 (PPB) contain the supplementary crystallographic data for this paper. These data can be obtained free of charge from The Cambridge Crystallographic Data Centre via www.ccdc.cam.ac.uk/data_request/cif

Acknowledgements

This work was partly supported by Grant-in-Aid (A) (No. 19205006) from the Ministry of Education, Culture, Sports, Science and Technology, Japan (A.O.), and the Star Faculty and BK21 Programs of the Ministry of Education and Human Resources of Korea (D.K.). Y.I. thanks the JSPS fellowship, and S.E. and J.M.L. thank the BK21 fellowships.

[1] a) T. Torres, *Angew. Chem.* **2006**, *118*, 2900–2903; *Angew. Chem. Int. Ed.* **2006**, *45*, 2834–2837; b) Y. Inokuma, A. Osuka, *Dalton Trans.* **2008**, 2517–2526.

[2] Y. Inokuma, J. H. Kwon, T. K. Ahn, M.-C. Yoon, D. Kim, A. Osuka, *Angew. Chem.* **2006**, *118*, 975–978; *Angew. Chem. Int. Ed.* **2006**, *45*, 961–964.

[3] A. Meller, A. Ossko, *Monatsh. Chem.* **1972**, *103*, 150–155.

[4] C. G. Claessens, D. González-Rodoríguez, T. Torres, *Chem. Rev.* **2002**, *102*, 835–853.

[5] a) N. Kobayashi, Y. Takeuchi, A. Matsuda, *Angew. Chem.* **2007**, *119*, 772–774; *Angew. Chem. Int. Ed.* **2007**, *46*, 758–760; b) Y. Takeuchi, A. Matsuda, N. Kobayashi, *J. Am. Chem. Soc.* **2007**, *129*, 8271–8281; c) E. A. Makarova, S. Shimizu, A. Matsuda, E. A. Luk'yanets, N. Kobayashi, *Chem. Commun.* **2008**, 2109–2111.

[6] a) Y. Inokuma, Z. S. Yoon, D. Kim, A. Osuka, *J. Am. Chem. Soc.* **2007**, *129*, 4747–4761; b) Y. Inokuma, A. Osuka, *Chem. Commun.* **2007**, 2938–2940; c) E. Tsurumaki, S. Saito, K. S. Kim, J. M. Lim, Y. Inokuma, D. Kim, A. Osuka, *J. Am. Chem. Soc.* **2008**, *130*, 438–439; d) Y. Inokuma, S. Easwaramoorthi, S. Y. Jang, K. S. Kim, D. Kim, A. Osuka, *Angew. Chem.* **2008**, *120*, 4918–4921; *Angew. Chem. Int. Ed.* **2008**, *47*, 4840–4843.

[7] T. Xu, R. Lu, X. Liu, P. Chen, X. Qiu, Y. Zhao, *Eur. J. Org. Chem.* **2008**, 1065–1071.

[8] Porphyrin perbromination: a) P. Bhyrappa, V. Krishnan, *Inorg. Chem.* **1991**, *30*, 239–245; b) P. Hoffmann, G. Labat, A. Robert, B. Meinier, *Tetrahedron Lett.* **1990**, *31*, 1991–1994; c) T. G. Traylor, S. Tsuchiya, *Inorg. Chem.* **1987**, *26*, 1338–1339; d) T. Wijesekera, A.

Matsumoto, D. Dolphin, D. Lexa. *Angew. Chem.* **1990**, *102, 1073–1074; Angew. Chem. Int. Ed. Engl.* **1990**, 29, 1028–1030; *Angew. Chem. Int. Ed. Engl.* **1990**, *29*, 1028–1030.

[9] Perethynylated porphyrins. T. Chandra, B. J. Kraft, J. C. Huffman, J. M. Zaleski, *Inorg. Chem.* **2003**, *42*, 5158–5172.

[10] K. M. Kadish, M. Lin, E. V. Caemelbecke, G. D. Stefano, C. J. Medforth, D. J. Nurco, N. Y. Nelson, B. Krattinger, C. M. Muzzi, L, Jaquinod, Y. Xu, D. C. Shyr, K. M. Smith, J. A. Shelnutt, *Inorg. Chem.* **2002**, *41*, 6673–6687.

[11] a) C. J. Medforth, K. M. Smith, *Tetrahedron Lett.* **1990**, *31*, 5583–5586; b) J. Takeda, T. Ohya, M. Sato, *Chem. Phys. Lett.* **1991**, *183*, 384–386; c) J. Takeda, T. Ohya, M. Sato, *Inorg. Chem.* **1992**, *31*, 2877–2880; d) J. Takeda, M. Sato, *Chem. Lett.* **1995**, 939–940; e) K. S. Chan, X. Zhou, B.-S. Luo, T. C. W. Mak, *J. Chem. Soc. Chem. Commun.* **1994**, 271–272; f) X. Zhou, Z.-Y. Zhou, T. C. W. Mak, K. S. Chan, *J. Chem. Soc. Perkin Trans* **1994**, 2519–2520; g) R. E. Haddad, S. Gazeau, J. Pecaut, J.-C. Marchon, C. J. Medforth, J. M. Shelnutt, *J. Am. Chem. Soc.* **2003**, *125*, 1253–1268; h) C. J. Medforth, R. E. Haddad, C. M. Muzzi, N. R. Dooley, L. Jaquinod, D. C. Shyr, D. J. Nurro, M. M. Olmstead, K. M. Smith, J.-G. Ma, J. A. Shelnett, *Inorg. Chem.* **2003**, *42*, 2227–2241.

[12] Peripherally fabricated subphthalocyanines: a) C. G. Claessens, T. Torres, *Angew. Chem.* **2002**, *114*, 2673–2677; *Angew. Chem. Int. Ed.* **2002**, *41*, 2561–2565; b) T. Fukuda, J. R. Stork, R. J. Potucek, M. M. Olmstead, B. C. Noll, N. Kobayashi, W. S. Durfee, *Angew. Chem.* **2002**, *114*, 2677–2680; *Angew. Chem. Int. Ed.* **2002**, *41*, 2565–2568; c) C. G. Claessens, T. Torres, *Chem. Eur. J.* **2000**, *6*, 2168–2172; d) N. Kobayashi, T. Nonomura, *Tetrahedron Lett.* **2002**, *43*, 4253–4255.

[13] Peripherally fabricated subporphyrazines: M. S. Rodríguez-Morgade, S. Esperanza, T. Torres, J. Barberá, *Chem. Eur. J.* **2005**, *11*, 354–360.

[14] a) M. V. Martinez-Diaz, M. Quintiliani, T. Torres, *Synlett* **2008**, 1–20; b) R. S. Iglesias, C. G. Claessens, M. Á. Herranz, T. Torres, *Org. Lett.* **2007**, *9*, 5381–5384.

[15] a) P. Szarvas, B. Györi, J. Emri, *Acta Chim. (Budapest)* **1971**, *70*, 1–8; b) R. Köster, H. Bellut, S. Hattori, *Liebigs Ann. Chem.* **1968**, *720*, 1–22.

[16] The Sonogashira-couplings of *meso*-halogenated porphyrins and trimethylsilyl acetylene, which provide *meso*-enyne-subsitituted porphyrins, were reported; Y.-J. Chen, G.-H. Lee, S.-M. Peng, C.-Y. Yeh, *Tetrahedron Lett.* **2005**, *46*, 1541–1544.

[17] M. Gouterman, *J. Mol. Spectrosc.* **1961**, *6*, 138–163.

[18] a) T. K. Ahn, K. S. Kim, D. Y. Kim, S. B. Noh, N. Aratani, C. Ikeda, A. Osuka, D. Kim, *J. Am. Chem. Soc.* **2006**, *128*, 1700–1704; b) M. Drobizhev, Y. Stepanenko, Y. Dzenis, A. Karotki, A. Rebane, P. N. Taylor, H. L. Anderson, *J. Am. Chem. Soc.* **2004**, *126*, 15352–15353; c) O.-K. Kim, K.-S. Lee, H. Y. Woo, K.-S. Kim, G. S. He, J. Swiatkiewicz, P. N. Prasad, *Chem. Mater.* **2000**, *12*, 284–286.

[19] M. Sheik-Bahae, A. A. Said, T.-H. Wei, D. J. Hagan, E. W. van Stryland, *IEEE J. Quantum Electron.* **1990**, *26*, 760–769.

[20] a) T. K. Ahn, J. H. Kwon, D. Y. Kim, D. W. Cho, D. H. Jeong, S. K. Kim, M. Suzuki, S. Shimizu, A. Osuka, D, Kim, *J. Am. Chem. Soc.* **2005**, *127*, 12856–12861; b) Z. S. Yoon, J. H. Kwon, M.-C. Yoon, M. K. Koh, S. B. Noh, J. L. Sessler, J. T. Lee, D. Seidel, A. Aguilar, S. Shimizu, M. Suzuki, A. Osuka, D. Kim, *J. Am. Chem. Soc.* **2006**, *128*, 14128–14134; c) I. Hisaki, S. Hiroto, K. S. Kim, S. B. Noh, D. Kim, H. Shinokubo, A. Osuka. *Angew. Chem.* **2007**, *119, 5217–5220; Angew. Chem. Int. Ed.* **2007**, 46, 5125–5128; *Angew. Chem. Int. Ed.* **2007**, *46*, 5125–5128; d) S. Mori, K. S. Kim, Z. S. Yoon, S. B. Noh, D. Kim, A. Osuka, *J. Am. Chem. Soc.* **2007**, *129*, 11344–11345; e) J. Song, S. Y. Jang, S. Yamaguchi, J. Sankar, S. Hiroto, N. Aratani, J.-Y. Shin, S. Easwaramoorthi, K. S. Kim, D. Kim, H. Shinokubo, A. Osuka. *Angew. Chem.* **2008**, *120, 6093–6096; Angew. Chem. Int. Ed.* **2008**, 47, 6004–6007; *Angew. Chem. Int. Ed.* **2008**, *47*, 6004–6007; f) M.-C. Yoon, S. B. Noh, A. Tsuda, Y. Nakamura, A. Osuka, D. Kim, *J. Am. Chem. Soc.* **2007**, *129*, 10080–10081; g) Y. Tanaka, S. Saito, S. Mori, N. Aratani, H. Shinokubo, N. Shibata, Y. Higuchi, Z. S. Yoon, K. S. Kim, S. B. Noh, J. K. Park, D. Kim, A. Osuka. *Angew. Chem.* **2008**, *120, 693–696; Angew. Chem. Int. Ed.* **2008**, 47, 681–684; *Angew. Chem. Int. Ed.* **2008**, *47*, 681–684; h) Y. Nakamura, S. Y. Jang, T. Tanaka, N. Aratani, J. M. Lim, K. S. Kim, D. Kim, A. Osuka, *Chem. Eur. J.* **2008**, *14*, 8279–8289.

[21] a) G. S. He, L-S. Tan, Q. Cheng, P. N. Prasad, *Chem. Rev.* **2008**, *108*, 1245–1330; b) O. Varnavski, X. Yan, O. Mongin, M. Blanchard-Desce, T. Goodson III, *J. Phys. Chem. C* **2007**, *111*, 149–162.

[22] a) B. R. Cho, K. H. Son, S. H. Lee, Y.-S. Song, Y.-K. Lee, S.-J. Jeon, J. H. Choi, H. Lee, M. Cho, *J. Am. Chem. Soc.* **2001**, *123*, 10039–10045; b) J. Zyss, *J. Chem. Phys.* **1993**, *98*, 6583–6599; c) A. Sastre, T. Torres, M. A. Diaz-Garcia, F. Agullo-Lopez, C. Dhenaut, S. Brasselet, I. Ledoux, J. Zyss, *J. Am. Chem. Soc.* **1996**, *118*, 2746–2747; d) J. Brunel, O. Mongin, A. Jutand, I. Kedoux, J. Zyss, M. Blanchard-Desce, *Chem. Mater.* **2003**, *15*, 4139–4148

[23] Gaussian 03, Revision B05, M. J. Frisch, G. W. Trucks, H. B. Schlegel, G. E. Scuseria, M. A. Robb, J. R. Cheeseman, J. A. Montgomery, Jr., T. Vreven, K. N. Kudin, J. C. Burant, J. M. Millam, S. S. Iyengar, J. Tomasi, V. Barone, B. Mennucci, M. Cossi, G. Scalmani, N. Rega, G. A. Petersson, H. Nakatsuji, M. Hada, M. Ehara, K. Toyota, R. Fukuda, J. Hasegawa, M. Ishida, T. Nakajima, Y. Honda, O. Kitao, H. Nakai, M. Klene, X. Li, J. E. Knox, H. P. Hratchian, J. B. Cross, V. Bakken, C. Adamo, J. Jaramillo, R. Gomperts, R. E. Stratmann, O. Yazyev, A. J. Austin, R. Cammi, C. Pomelli, J. W. Ochterski, P. Y. Ayala, K. Morokuma, G. A. Voth, P. Salvador, J. J. Dannenberg, V. G. Zakrzewski, S. Dapprich, A. D. Daniels, M. C. Strain, O. Farkas, D. K. Malick, A. D. Rabuck, K. Raghavachari, J. B. Foresman, J. V. Ortiz, Q. Cui, A. G. Baboul, S. Clifford, J. Cioslowski, B. B. Stefanov, G. Liu, A. Liashenko, P. Piskorz, I. Komaromi, R. L. Martin, D. J. Fox, T. Keith, M. A. Al-Laham, C. Y. Peng, A. Nanayakkara, M. Challacombe, P. M. W. Gill, B. Johnson, W. Chen, M. W. Wong, C. Gonzalez, J. A. Pople, Gaussian, Inc., Wallingford CT, **2004**

[24] A. Altomare, M. C. Burla, M. Camalli, G. L. Cascarano, C. Giacovazzo, A. Guagliardi, A. G. G. Moliterni, G. Polidori, R. Spagna, *J. Appl. Crystallogr.* **1999**, *32*, 115–119.

[25] SHELXL-97 and SHELXS-97, program for refinement of crystal structures from diffraction data, University of Göttingen, Göttingen (Germany); G. M. Sheldrick, T. R. Schneider, *Methods Enzymol.* **1997**, *277*, 319–343.

Received: September 2, 2008
Published online: December 4, 2008

